Granular Gases of Rod-Shaped Grains in Microgravity

K. Harth,[1] U. Kornek,[1] T. Trittel,[1] U. Strachauer,[1] S. Höme,[2] K. Will,[3] and R. Stannarius[1]

[1]*Institute of Experimental Physics, Otto-von-Guericke Universität Magdeburg, D-39016 Magdeburg, Germany*
[2]*Institute of Automation Engineering, Otto-von-Guericke Universität Magdeburg, D-39016 Magdeburg, Germany*
[3]*Institute for Electronics, Signal Processing and Communications, Otto-von-Guericke Universität Magdeburg, D-39016 Magdeburg, Germany*

(Received 17 September 2012; published 2 April 2013)

Granular gases are convenient model systems to investigate the statistical physics of nonequilibrium systems. In the literature, one finds numerous theoretical predictions, but only few experiments. We study a weakly excited dilute gas of rods, confined in a cuboid container in microgravity during a suborbital rocket flight. With respect to a gas of spherical grains at comparable filling fraction, the mean free path is considerably reduced. This guarantees a dominance of grain-grain collisions over grain-wall collisions. No clustering was observed, unlike in similar experiments with spherical grains. Rod positions and orientations were determined and tracked. Translational and rotational velocity distributions are non-Gaussian. Equipartition of kinetic energy between translations and rotations is violated.

DOI: 10.1103/PhysRevLett.110.144102 PACS numbers: 05.45.−a, 45.50.−j, 81.70.Ha, 83.10.Pp

Fluidized granulates represent one of the most fundamental and fascinating systems to elucidate statistical physics in steady states far from thermal equilibrium. Granular gases are agitated dilute ensembles of macroscopic grains. Visually, they strongly resemble our mental image of molecular gases, but the dissipative nature of grain collisions leads to qualitative differences in molecular gas behavior. Clustering instabilities [1–4], non-Gaussian velocity distributions of the grains [4–11], coupling of rotational and translational motions [12], and anomalous scaling of the pressure [3,13] represent striking features. We demonstrate that granular gases of rodlike grains open new opportunities to study the dynamics of nonequilibrium statistical ensembles.

The literature comprises numerous analytical and numerical predictions on granular gases, based on the same assumptions of grain interactions. Experimental results are partially conflicting even on basic characteristics. Minimizing the bias from strong driving or substrate interactions in experiments is crucial for a clear interpretation of the results. Previous microgravity [9,10,14] or levitation [6,7,15] experiments focussed on two-dimensional (2D) ensembles of spheres. In 3D samples, clustering occurs already at low filling fractions [2,3], individual grain dynamics were only obtained in the Knudsen-regime [16]. Detailed dynamics in grain-grain collision dominated gases were not accessible.

Real granulates are often composed of nonspherical grains—and the effective shape of the constituents can lead to anisotropic collective properties in various soft matter systems [17]. In granulates, phenomena like orientational order [18], giant density fluctuations [19] or flow alignment [20] were reported. We study a granular gas of rod-shaped grains in 3D. It offers substantial experimental advantages over spheres: Due to a significantly shorter mean free path at comparable filling fraction, we obtain a granular gas in a homogeneous steady state in the grain-grain collision dominated regime at weak external excitation. We are able to resolve the translational and rotational motion of all individual grains.

Theoretical results on granular gases of elongated particles suggest that equipartition is violated in general [21–25]. Clusters were predicted to be unstable [22,23]. Specific characteristics of the granular gas depend on the aspect ratio, shape, and mass distribution of the grains. Previous experiments were focused on strongly driven or 2D systems, often with low numbers of particles. Rods in an air-fluidized layer were shown to exhibit anisotropy in the translations along and perpendicular to the rod symmetry axis [26], and waves propagate at an increased velocity in such systems [27]. Granular gases of dimers confined to a 2D layer showed a normal distribution of velocities in bulk in good approximation [24,28]. Influences of the shaking parameters were studied [29]. Large boundary effects on grain dynamics were demonstrated for such systems [30].

The presented experiments were performed during a sounding rocket flight (REXUS 10, suitable microgravity period ≈ 70 s, remaining accelerations $<0.01g$). An ensemble of $N = 250$ differently colored cylinders of equal size (insulated copper wire, length $L = 1.2$ cm, diameter $d = 0.13$ cm) was confined in a container of volume $V = 535.5\ \mathrm{cm}^3$ (filling fraction $\approx 0.74\%$). Their mean free path λ is essentially related to the grain length L,

$$\lambda \approx \frac{4\sqrt{2}}{\pi}\frac{V}{NL^2} \approx 2.6\ \mathrm{cm}. \quad (1)$$

The mass of a single rod is $m = 0.045$ g, and moments of inertia are $J_{\parallel} = 5.4 \times 10^{-12}\,\mathrm{kgm}^2$ and $J_{\perp} = 545 \times 10^{-12}\,\mathrm{kgm}^2$ for rotation axes parallel and perpendicular to the symmetry axis, respectively. Front and top walls of the container [Fig. 1(a)] consist of acrylic glass, the side walls are aluminum. Two side walls and the back wall were agitated sinusoidally using voice-coil actuators. The side

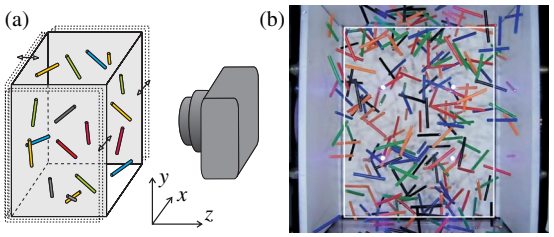

FIG. 1 (color online). (a) Schematic experimental setup and selected coordinate system: container with 3 moveable walls agitated by voice-coil actuators, width: 8.5 cm, height 10 cm, depth 6.3 cm, top camera not shown; (b) freeze frame of the granular gas of 250 colored rods excited by shaking side walls (30 Hz) in microgravity. The white box indicates the region selected for statistical evaluation. See Supplemental Material [32] for movies of the granular gas.

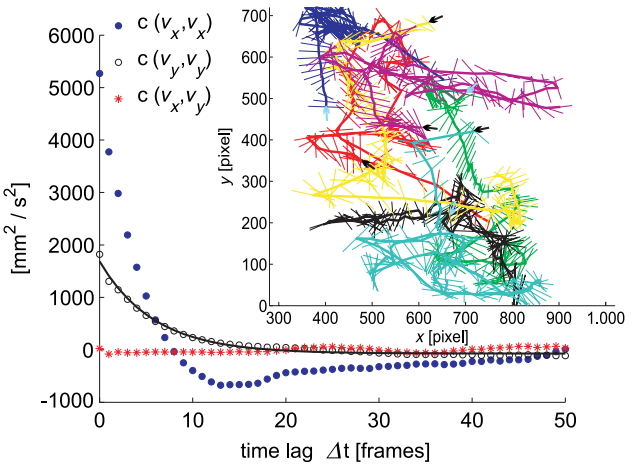

FIG. 2 (color online). Temporal autocorrelation and cross correlation of the translational velocities in the direct excitation direction (x) in the indirectly excited direction (y) at Excitation (1). The inset shows exemplary rod trajectories over 101 frames, arrows indicate the beginning.

walls move in antiphase. Two excitation strengths were examined (see Table I, corresponding peak accelerations $\Gamma(1) = 3.7g$, $\Gamma(2) = 2.9g$). The container was front-illuminated with four high-power LEDs. The observation from front and top was realized using two commercial digital compact cameras (SAMSUNG PL70, 29.4 fps at 1280×720 pixel), see Ref. [31] for details. Within this study, the top view images were used to verify the uniform distribution of particles in the container. The z positions of the particles were not evaluated. A scale of 0.1412 mm/pixel in the video refers to the midplane of the box in the field of view. Distances and velocities appear 20% larger in the front plane, and 20% smaller in the back plane.

Unambiguous automatic particle tracking could not be achieved due to the limited time resolution, therefore all rods were tracked manually. Special care has been taken to ensure that each particle in a frame was correctly detected and assigned. In order to find a reasonable compromise between satisfactory statistics and manageable evaluation efforts, we have restricted ourselves here to 2D tracking of two representative frame sequences. The front view images alone yield valuable information on the characteristics of the ensemble. The results presented in this Letter were obtained from two sequences of 101 frames in front view (each $\approx 25\,000$ out of half a million available data points). To minimize boundary effects, only rods with centers of mass in the central region [see Fig. 1(b)] entered the velocity statistics. A second set of evaluated sequences yielded similar results.

The rods distribute evenly in the x-y plane (Fig. 1(b) and video [32]), with small transient density fluctuations. Typical trajectories are shown in Fig. 2. We note that in the data analysis, we make a qualitative distinction between the x direction, which is enclosed laterally by shaking walls, and the y direction, which is enclosed by fixed walls. Momentum exchange with the container is different for these two directions. Temporal autocorrelations and cross correlations $c(v_i, v_j)$ for the particle velocities are shown in Fig. 2. The two translational degrees of freedom are uncorrelated, as expected. The autocorrelation of v_y decreases exponentially with decay time ≈ 0.2 s. In excitation direction, x, we find positive autocorrelations over ≈ 8 frames (0.27 s). Thereafter, velocities are slightly anticorrelated. These graphs evidence that the temporal resolution of our measurement is sufficient to obtain relevant statistics of the gas dynamics. It is also evident that the two spatial directions are not equivalent, as discussed above.

Figure 3 shows the velocity distributions of all rods in the selected region for Excitation (1), parameters see Table I. Due to the perspective view (see above), measured velocity distributions are an average of apparent velocity distributions from different depths. It turns out that this averaging results in a distribution that is very close to the true distribution in the container midplane (in z direction). Deviations are negligible with respect to the statistical error in the experimental data. Moments and other characteristics of the distributions calculated from the data sets are listed in Table I. The mean of each data set, μ, is a measure for net external accelerations (deviations of the container trajectory from $0g$). These deviations are more than 1 order of magnitude smaller than the mean absolute velocities and angular velocities, respectively, and thus negligible.

In earlier work on nonspherical particles, nearly Gaussian velocity distributions were found [24,28]. Indeed, the distribution of v_y can be satisfactorily approximated by a Gaussian [Fig. 3(a)]. Deviations occur mainly near the maximum where we find some excess of slow grains. Only slight high-velocity tails are present. The distribution of v_x is clearly non-Gaussian with pronounced high-velocity tails. Still, the central part of the distribution of v_x is not too different from a Gaussian (Fig. 3, bottom). The solid curve corresponds to the parameters for v_y in Table I. For both velocity components, the distributions are somewhat better described by a probability density $\propto \exp\{-(|v_i - \mu|/C)^\beta\}$ with $\beta = 1.5$. A similar value was found in 2D experiments with spherical grains [7–9].

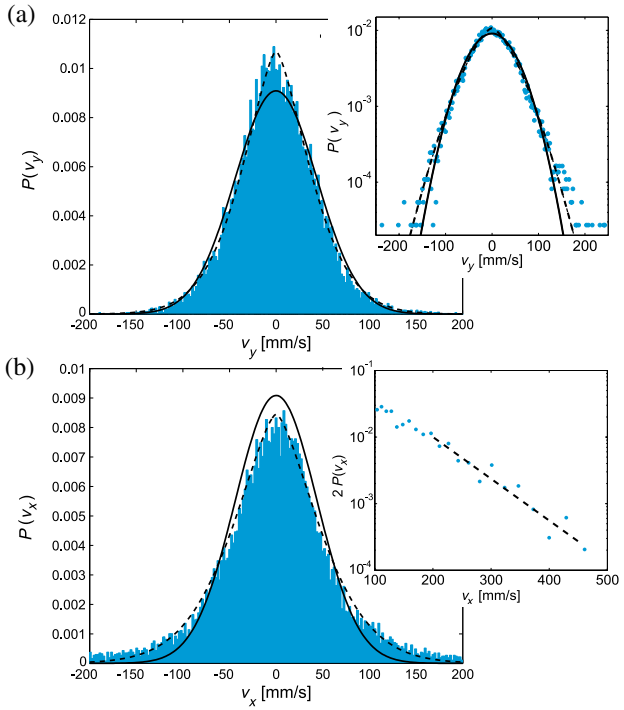

FIG. 3 (color online). Translational velocity distributions at Excitation (1), obtained from 101 frames with 250 particles each. The inset of (a) shows the same data in a logarithmic plot, the inset of (b) displays the tails of the distribution of $|v_x|$ in a logarithmic plot. Shaded areas, dots in the insets: data histogram, solid lines: Gaussians with (μ_i, σ_y), see Table I, dashed lines in main figures and inset of (a): non-Gaussian distributions $P(v_y) = 0.0107\exp\{-(|v_y - \mu_y|/51.77\ \mathrm{m/s})^{1.5}\}$ and $P(v_x) = 0.008457\exp\{-(|v_x - \mu_x|/65.49\ \mathrm{m/s})^{1.5}\}$, respectively, the dashed line is a guide to the eye and corresponds to a velocity distribution $\propto \exp\{-(v_x - \mu_x)/C\}$.

The v_y distribution is well fitted in the whole velocity range. For the direct excitation direction, v_x, prominent tails scaling with an exponent $\beta \approx 1$ are present. In previous work with spherical grains, Gaussian distributions ($\beta = 2$) were found in specific situations [11,33]. Distributions with other scalings ($1 \leq \beta < 2$, $\beta \neq 1.5$) were observed depending on driving and substrate interactions. The distributions were often compared to analytical results in the high-velocity limit [34], which is usually not reached in experiments [35]. The existence of tails can be partially attributed to wall interactions. In the case of rodlike grains, the wall interaction mechanisms are far more complex than for spherical grains: a distribution of post-collision translational and rotational energies dependent on the impact angle is found even for single rods bouncing on a vibrating plate [36]. Thus, it is questionable to draw an analog to driven granular gases of spherical grains based on the energy input from flat vibrating plates. Significantly smaller deviations from a Gaussian distribution are expected.

While the translational directions are clearly separated in the 2D view, a separation of the rotational degrees of freedom is not straightforward. As we observe a 2D projection, while the rods rotate in 3D, special care must be taken to separate the components of particle rotations. We employ a standard technique [37]: only rotational velocities ω of rods whose length of the projection does not change within a tolerance of $\pm 5\%$ in subsequent frames are considered. Thus we select only the subset of particles whose momentary rotation axis is parallel to the viewing direction, their average rotation energy is thus equal to the complete mean energy of the two rotational degrees of freedom about the short rod axes. The distribution of the rotational velocities at Excitation (1) is shown in Fig. 4. Again, the distribution is non-Gaussian and well described by a probability density $\propto \exp\{-(|\omega - \mu_\omega|/C)^{1.5}\}$. Deviations at high angular velocities are present.

TABLE I. Excitation parameters (frequency f and mean peak-peak amplitude A) and calculated statistical quantities (mean μ, standard deviation σ, mean absolute value, mean energy per rod) for the analyzed velocity and angular velocity distributions, the second column contains the number of data points n over which the averages are taken. The last column gives the corresponding kinetic energy per particle and degree of freedom. The absolute mean and μ are given in mm/s (v_x, v_y) and deg/s(ω), σ is given in mm/s (v_x, v_y) and deg/s(ω), E is given in nJ. Excitation (1): $f =$ 30 Hz, $A = 2.05$ mm; Excitation (2): $f = 20$ Hz, $A = 3.65$ mm.

		n	μ	σ	Abs. mean	E
Excitation (1)	v_x	17 705	2.1	70.8	49.6	112.6
	v_y	17 705	−1.8	43.9	33.8	43.4
	ω	4712	15.6	733	543	22.3
Excitation (2)	v_x	17 210	1.0	73.4	51.7	121.1
	v_y	17 210	−0.9	48.7	37.3	53.3
	ω	4512	15.7	757	561	23.8

The characteristic features of the velocity and angular velocity distributions, i.e., their shapes, the existence and scaling of tails, are qualitatively similar at both Excitations (1) and (2). Therefore, graphs for Excitation (2) are omitted here. In general, the second excitation yields larger mean absolute and squared velocities, see Table I.

Interactions with the container walls are important parameters of the energy balance. We have estimated the energy losses during collisions with fixed walls from the statistics of drop experiments. Rods with random initial orientations were dropped onto a horizontal aluminum plate. Velocities and rotations were extracted from high-speed videos. The energy dissipated in a collision depends on the impact angle [24], and the bouncing dynamics are much more complex than for spheres [36,38]. From a statistics of 500 drops we found that on average 71% of the kinetic energy is dissipated. After collision, 22% of the initial energy remains in the vertical motion, 1% is transformed into horizontal motion and 6% into rotational energy.

For a dilute gas, the energy input cannot easily be related to the peak acceleration of the vibrating plates. An estimation of the mean energy of rods on a vibrating plate was given by Wright *et al.* [36]. They reported a distribution of the total energies after the collisions (which is, strictly, not

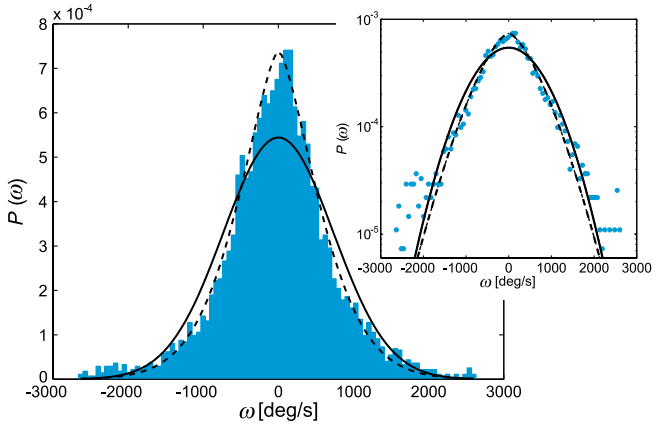

FIG. 4 (color online). Rotational velocity distribution at Excitation (1). Solid line: Gaussian with the parameters for ω from Table I, dashed curve: $P(\omega) = 0.00074\exp\{-(|\omega - \mu_\omega|/748.5\ \text{deg/s})^{1.5}\}$.

the time-averaged energy) with exponential decay, yielding a mean energy proportional to $A^2 f^2$. This parameter would be $945\,\text{mm}^2\,\text{s}^{-2}$ for Excitation (1), and $1330\,\text{mm}^2\,\text{s}^{-2}$ for Excitation (2), suggesting a somewhat more efficient agitation in the latter case. This is confirmed at least qualitatively in our experiments (Table I).

The distribution of energy onto the different degrees of freedom is of particular interest. The kinetic energies per particle in the translational degrees of freedom are calculated as $E_{x,y} = m\sigma^2_{x,y}/2$. With our evaluation procedure, we obtain the full rotational energy per particle for rotations around axes perpendicular to the symmetry axis as $E_\omega = J_\perp \sigma^2_\omega/2$. This value corresponds to two rotational degrees of freedom (see above). The averaged energies can be interpreted as granular temperatures. Figure 5 shows the energies for each evaluated frame. The relative fluctuations of E_x are significantly larger than those of E_y. Larger fluctuations in E_ω are due to poorer statistics. The temporal fluctuations of the energies are on the time scale of the average particle collision rates (decay times of the autocorrelations in Fig. 2). The translational degree of freedom along x [$E_x \approx 2.5\,E_y$, see Table I and Fig. 5(a)] is much stronger excited due to energy input from vibrating side walls. This excess energy is gradually distributed to all degrees of freedom by rod-rod collisions. The statistics for Excitation (2), Fig. 5(b), yield essentially the same features for E_y and E_ω, with slightly higher means (Table I). We find a clear excess of translational over rotational energy per degree of freedom, see Table I, qualitatively predicted by numerical simulations during granular cooling [22,25]. The approximate equality of rotational and translational energy in previous 2D experiments [26] may be caused by evident coupling of rotations and translations at their substantially larger area fractions and 2D confinement.

Summarizing, we presented the first experimental study of a weakly excited 3D granular gas of rodlike grains. The rods distribute evenly in the container, no noticeable clustering was observed. The mean free path is much shorter

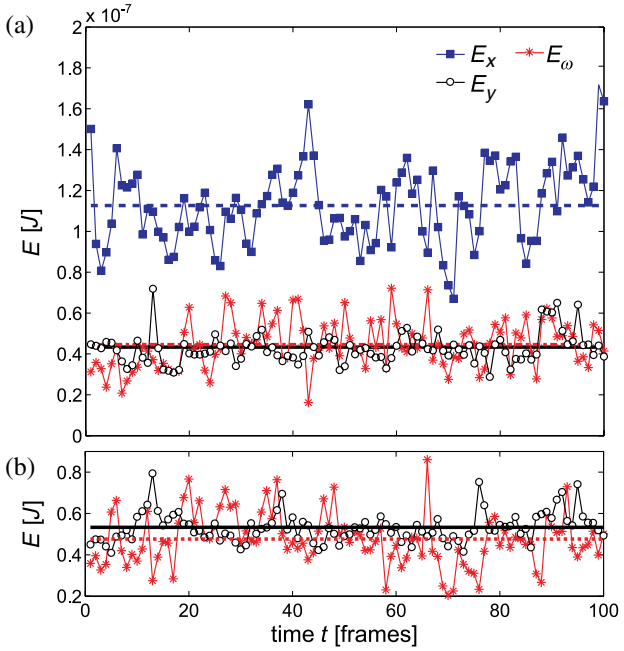

FIG. 5 (color online). Energies $E(t)$ in the observed degrees of freedom for the 30 Hz (a) and 20 Hz (b) excitations. Horizontal lines reflect the time averages from Table I. For the 20 Hz excitation, the E_x curve is qualitatively similar to that for 30 Hz in (a).

than that of granular gases of spherical grains at a comparable filling fraction. The distributions of translational and rotational velocities were determined. While the velocity distribution in the direction that is only indirectly excited through rod-rod collisions remains fairly close to a Gaussian, the distribution of velocities in the excitation direction as well as the distribution of the rotational velocities are clearly non-Gaussian. All distributions are better approximated by stretched exponentials $\propto \exp\{-(|v_i - \mu_i|/C)^{1.5}\}$. Significant high-velocity tails are found for the translational motion in excitation direction x, with an approximate scaling $\propto \exp\{-(|v_x - \mu_x|/D)\}$. Somewhat weaker tails exist in the rotational velocity ω and translations in the y direction excited by grain-grain collisions. Equipartition of the energies between translational and rotational motion is violated. The ratio of the total energies in the two excitation schemes is consistent with the assumption of an excitation efficiency proportional to $A^2 f^2$. This would agree with the findings for single rodlike grains [36], but one has to be cautious due to a different definition of the mean total energy there. For spherical grains, such scaling was reported for high excitation strengths only [39].

Although granular gases of rodlike grains may at first glance introduce additional complications into granular dynamics, they open in fact promising possibilities to access new insights that are hardly achievable in experiments with spheres, viz., dynamics of grain-grain collision dominated regimes in 3D with detailed particle tracking of rotations and translations. Boundary interactions introduce less coherence into the ensemble [36]. Exploring the effects of shape, aspect ratio, filling fraction, excitation parameters

or material properties on the dynamics is possible. The study of granular gases of rodlike grains may substantially improve our understanding of *real* granular systems.

The German Aerospace Center DLR, ESA, and SSC staffs are cordially acknowledged for excellent assistance throughout the REXUS campaign. K. Daniels, I. Aranson and P. Evesque are kindly acknowledged for helpful comments. DLR, SNSB and ESA are acknowledged for funding within the REXUS/BEXUS program, project GAGa. DLR is acknowledged for partial funding in project 50WM1127.

[1] I. Goldhirsch and G. Zanetti, Phys. Rev. Lett. **70**, 1619 (1993); A. Kudrolli, M. Wolpert, and J. P. Gollub, Phys. Rev. Lett. **78**, 1383 (1997); M. V. Sapozhnikov, I. S. Aranson, and J. S. Olafsen, Phys. Rev. E **67**, 010302 (2003); E. Opsomer, F. Ludewig, and N. Vandewalle, Phys. Rev. E **84**, 051306 (2011).

[2] E. Falcon, R. Wunenburger, P. Évesque, S. Fauve, C. Chabot, Y. Garrabos, and D. Beysens, Phys. Rev. Lett. **83**, 440 (1999).

[3] E. Falcon, S. Aumaître, P. Évesque, F. Palencia, C. Lecoutre-Chabot, S. Fauve, D. Beysens, and Y. Garrabos, Eur. Biophys. J. **74**, 830 (2006).

[4] J. S. Olafsen and J. S. Urbach, Phys. Rev. Lett. **81**, 4369 (1998).

[5] J. S. Olafsen and J. S. Urbach, Phys. Rev. E **60**, R2468 (1999); A. Kudrolli and J. Henry, Phys. Rev. E **62**, R1489 (2000); K. Nichol and K. E. Daniels, Phys. Rev. Lett. **108**, 018001 (2012); M. Schmick and M. Markus, Phys. Rev. E **78**, 010302 (2008).

[6] K. Kohlstedt, A. Snezhko, M. Sapozhnikov, I. Aranson, J. Olafsen, and E. Ben-Naim, Phys. Rev. Lett. **95**, 068001 (2005).

[7] I. S. Aranson and J. S. Olafsen, Phys. Rev. E **66**, 061302 (2002).

[8] F. Rouyer and N. Menon, Phys. Rev. Lett. **85**, 3676 (2000); W. Losert, D. G. W. Cooper, J. Delour, A. Kudrolli, and J. P. Gollub, Chaos **9**, 682 (1999).

[9] S. Tatsumi, Y. Murayama, H. Hayakawa, and M. Sano, J. Fluid Mech. **641**, 521 (2009).

[10] M. Hou, R. Liu, G. Zhai, Z. Sun, K. Lu, Y. Garrabos, and P. Evesque, Microgravity Sci. Technol. **20**, 73 (2008).

[11] C. Huan, X. Yang, D. Candela, R. Mair, and R. Walsworth, Phys. Rev. E **69**, 041302 (2004).

[12] M. Huthmann and A. Zippelius, Phys. Rev. E **56**, R6275 (1997); N. V. Brilliantov, T. Pöschel, W. T. Kranz, and A. Zippelius, Phys. Rev. Lett. **98**, 128001 (2007).

[13] J.-C. Geminard and C. Laroche, Phys. Rev. E **70**, 021301 (2004).

[14] Y. Grasselli, G. Bossis, and G. Goutallier, Eur. Biophys. J. **86**, 60 007 (2009); C. Yanpei, P. Evesque, M. Hou, C. Lecoutre, F. Palencia, and Y. Garrabos, J. Phys. Conf. Ser. **327**, 012033 (2011).

[15] C. C. Maaß, N. Isert, G. Maret, and C. M. Aegerter, Phys. Rev. Lett. **100**, 248001 (2008).

[16] P. Evesque, F. Palencia, C. Lecoutre-Chabot, D. Beysens, and Y. Garrabos, Microgravity Sci. Technol. **16**, 280 (2005).

[17] D. van der Beek, H. Reich, P. van der Schoot, M. Dijkstra, T. Schilling, R. Vink, M. Schmidt, R. van Roij, and H. Lekkerkerker, Phys. Rev. Lett. **97**, 087801 (2006); M. P. Lettinga and J. K. G. Dhont, J. Phys. Condens. Matter **16**, S3929 (2004); F. Peruani, A. Deutsch, and M. Bär, Phys. Rev. E **74**, 030904 (2006); A. Eremin, R. Stannarius, S. Klein, J. Heuer, and R. M. Richardson, Adv. Funct. Mater. **21**, 566 (2011); P. G. de Gennes and J. Prost, *The Physics of Liquid Crystals* (Clarendon Press, Oxford, 1993).

[18] J. Galanis, D. Harries, D. Sackett, W. Losert, and R. Nossal, Phys. Rev. Lett. **96**, 028002 (2006); V. Narayan, N. Menon, and S. Ramaswamy, J. Stat. Mech. (2006) P01005; D. L. Blair, T. Neicu, and A. Kudrolli, Phys. Rev. E **67**, 031303 (2003).

[19] V. Narayan, S. Ramaswamy, and N. Menon, Science **317**, 105 (2007); I. S. Aranson, A. Snezhko, J. S. Olafsen, and J. S. Urbach, Science **320**, 612c (2008); V. Narayan, S. Ramaswamy, and N. Menon, Science **320**, 612d (2008).

[20] I. S. Aranson, D. Volfson, and L. S. Tsimring, Phys. Rev. E **75**, 051301 (2007); T. Börzsönyi, B. Szabó, G. Törös, S. Wegner, J. Török, E. Somfai, T. Bien, and R. Stannarius, Phys. Rev. Lett. **108**, 228302 (2012); S. Wegner, T. Börzsönyi, T. Bien, G. Rose, and R. Stannarius, Soft Matter **8**, 10 950 (2012); T. Börzsönyi, B. Szabó, S. Wegner, K. Harth, J. Török, E. Somfai, T. Bien, and R. Stannarius, Phys. Rev. E **86**, 051304 (2012).

[21] T. Aspelmeier, G. Giese, and A. Zippelius, Phys. Rev. E **57**, 857 (1998).

[22] M. Huthmann, T. Aspelmeier, and A. Zippelius, Phys. Rev. E **60**, 654 (1999).

[23] T. Kanzaki, R. C. Hidalgo, D. Maza, and I. Pagonabarraga, J. Stat. Mech. (2010) P06020.

[24] G. Costantini, U. M. B. Marconi, G. Kalibaeva, and G. Cicotti, J. Chem. Phys. **122**, 164505 (2005).

[25] F. Villemot and J. Talbot, Granular Matter **14**, 91 (2012).

[26] L. J. Daniels, Y. Park, T. C. Lubensky, and D. J. Durian, Phys. Rev. E **79**, 041301 (2009).

[27] L. J. Daniels and D. J. Durian, Phys. Rev. E **83**, 061304 (2011).

[28] R. D. Wildman, J. Beecham, and T. L. Freeman, Eur. Phys. J. Special Topics **179**, 5 (2009).

[29] J. Atwell and J. S. Olafsen, Phys. Rev. E **71**, 062301 (2005).

[30] J. S. van Zon, J. Kreft, D. Goldman, D. Miracle, J. Swift, and H. Swinney, Phys. Rev. E **70**, 040301 (2004).

[31] K. Harth, S. Höme, T. Trittel, U. Kornek, U. Strachauer, and K. Will, in *Proceedings of 20th ESA Symposium on Rocket and Balloon Science* (European Space Ageny, Hyère, 2011), Report No. SP-700, p. 493.

[32] See Supplemental Material at http://link.aps.org/supplemental/10.1103/PhysRevLett.110.144102 for movies.

[33] G. W. Baxter and J. S. Olafsen, Nature (London) **425**, 680 (2003); Granular Matter **9**, 135 (2006).

[34] T. P. C. van Noije and M. H. Ernst, Granular Matter **1**, 57 (1998); S. E. Esipov and T. Pöschel, J. Stat. Phys. **86**, 1385 (1997).

[35] A. Barrat and E. Trizac, Eur. Phys. J. E **11**, 99 (2003).

[36] H. S. Wright, M. R. Swift, and P. J. King, Phys. Rev. E **74**, 061309 (2006).

[37] J. Blum, S. Bruns, D. Rademacher, A. Voss, B. Willenberg, and M. Krause, Phys. Rev. Lett. **97**, 230601 (2006).

[38] S. Dorbolo, D. Volfson, L. Tsimring, and A. Kudrolli, Phys. Rev. Lett. **95**, 044101 (2005).

[39] J.-C. Geminard and C. Laroche, Phys. Rev. E **68**, 031305 (2003).